Mechanical behavior of intact and remoulded calcareous silts

G.T. Lim
SRK Consulting (Australasia) Pty Ltd, Perth

N. Boukpeti & A. Fourie
The University of Western Australia, Perth

J.A. Pineda
The University of Newcastle, Newcastle

J.A.H. Carraro
Imperial College London, United Kingdom

ABSTRACT: Calcareous silts are encountered in many offshore areas where oil and gas exploitations are taking place (e.g., Arabian gulf, south east of Brazil, south east and north west of Australia). Understanding behavior of calcareous silts remains challenging as undisturbed silt samples are difficult to obtain, and most studies rely on remoulded silt samples. The purpose of this paper is to characterize the mechanical behavior of intact and remoulded offshore calcareous silts from two different water depths. The comparisons are done based on microstructure characterization using scanning electron microscopy (SEM) images supported by index tests, one-dimensional compression tests and undrained monotonic triaxial tests. The results have shown that, except for the critical state friction angle, the behaviour of remoulded silts differs from that of intact silts, due to the change in microstructure, which appears to be more compact with less intact open shell particles.

1 INTRODUCTION

Calcareous sediments are encountered in many offshore areas where oil and gas explorations are taking place (e.g., Arabian gulf, southern Brazil, south east and north-west regions of Australia). Previous research has shown that calcareous sediments are highly variable in composition and behaviour, ranging from cemented calcarenites, through uncemented sands and silty sands, calcareous muds and high-plasticity calcareous 'clays' (McClelland 1988; Nyland 1988; Price 1988). With offshore activities extending into deep water areas, the sediments that engineers have to build on are essentially fine-grained calcareous soils, with various amounts of silt and clay-sized particles.

While a significant amount of work has been published on the behaviour of cemented and uncemented calcareous sands (Carter et al. 1988; Coop 1990; Coop & Atkinson 1993; Sharma & Ismail 2006), knowledge of the response of fine-grained calcareous silts is still limited. Mao and Fahey (2003) investigated the behaviour of two calcareous silts with various amounts of clay-sized particles. Their study focused on the response in undrained cyclic simple shear tests of remoulded specimens. One of the silty material studied, had 60 % by weight of clay-sized particles ('muddy' silt), this silt was remoulded using a synthetic flocculant and heat treatment to reproduce the microstructure and behaviour of the natural soil. The results of monotonic undrained simple shear tests on normally consolidated specimens showed a contractive response, similar to the undisturbed soil. However, unflocculated specimens exhibited a dilative response, which may be attributed to a lower initial void ratio and a different soil structure. The second silt material studied was mixed with some commercially produced carbonate powder and silicon oil (resulting in 73% silt and 27% sand). For this silt, the undrained shear behaviour was dilative with strong strain hardening characteristics.

Previous studies have shown that various factors affect the shear behaviour of calcareous silty soils, such as the clay-sized fraction, initial void ratio, stress history and soil structure (Cola & Simonini 2002; Murthy et al. 2007; Anantanasakul et al. 2012). Recently, Lehane et al. (2014) compared the mechanical response of two carbonate sediments from Australia's North West Shelf and they have shown that fines content affects the undrained shear strength of these soils, by controlling the void ratio/density. However, published data on intact calcareous silty soils are still limited and there is a lack of guidance on how test results obtained from remoulded specimens may be used to infer the behaviour of intact soil. The aim of this paper is to make a contribution in this direction, by conducting an experimental program on intact and remoulded calcareous silty soils, which includes microscopic and mechanical soil characterisation.

2 SOIL TESTED AND EXPERIMENTRAL PROCEDURE

Two offshore natural calcareous silts from Western Australia were sampled using an 80 mm diameter piston tube sampler; Silt A from 575 m water depth and Silt B from 1341 m water depth. The samples were obtained from relatively shallow depth below the mudline, between 3 and 4 m. Both silts contained a significant amount of clay-size particles, or mud, as indicated by the particle size distribution (PSD) curves shown in Figure 1 (23 % for Silt A and 45 % for Silt B). Index properties such as *in situ* water content, Atterberg's limits, specific gravity and calcium carbonate ($CaCO_3$) content are listed in Table 1. For both silts, the natural water content was close to the liquid limit and the $CaCO_3$ content was greater than 75%. According to the Unified Soil Classification System (USCS), Silt A is classified as silt with traces of sand while Silt B is clayey silt. Both silts have high plasticity based on their Atterberg limits.

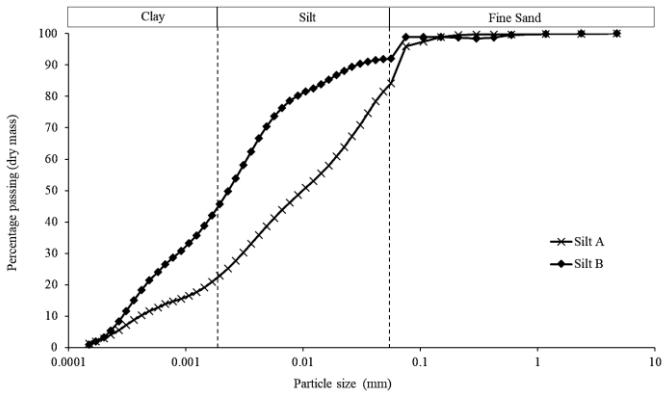

Figure 1: Particle size distribution of Silt A and Silt B

Table 1: Index properties of Silt A and Silt B

Silt	Water content, w_0	Liquid limit, w_L	Plasticity index, I_p	Specific gravity, G_s	Calcium carbonate content
	(%)	(%)	(%)	(-)	(%)
A	50.2	52.8	22.2	2.69	76.4
B	81.2	82.5	34.6	2.70	91.4

To prepare remoulded specimens of each soil, a slurry with a target water content of 1.2 times the liquid limit was prepared by mixing the original soil sample with deionised water. Next, the slurry was left for at least 12 hours and was mixed again before it was poured into a greased cylindrical consolidation tube with internal diameter of 72 mm. The silt slurry was then consolidated in stages up to 60 kPa until no further displacement was measured. The sample was extruded out from the tube and trimmed according to the required dimensions for each element test.

For microscopic characterisation, small cubes approximately 5 mm in size were cut from both intact and remoulded specimens. Scanning electron microscopy was done using Zeiss 1555 VP-FESEM to produce the SEM images, while X-ray crystallography was performed using Panalytical Empyrean XRD to identify the mineralogy of each soil.

One-dimensional compression tests using constant rate of strain (CRS) were carried out using a specimen size of 24 mm in height and 43 mm in diameter. Back pressure was applied at the top of the specimen while pore pressure was measured at the bottom. The specimens were loaded up to a maximum vertical stress of 1600 kPa using a strain rate of 1.85 %/hr and then unloaded at a rate of 2.4 %/h.

The triaxial tests were performed using a GDS Enterprise Level Dynamic (ELDYN) triaxial testing system. Triaxial specimens were prepared by extruding a sample from a 140 mm long section of sampling tube, which was then trimmed to a specimen of 105 mm in height and 50 mm in diameter. Various consolidation stresses were used, corresponding to either normally consolidated or over-consolidated states. The specimen was consolidated anisotropically (K_0 = 0.5) in two stages up to the selected stress state. In the first stage, the axial stress was increased until the state of stress reached the required K_0 value. In the second stage, a linear stress path was prescribed until the selected stresses were reached. Consolidation was considered complete when the excess pore pressure had fully dissipated and the axial strain rate was around 0.0035 %/day or less. At the end of consolidation, the specimen was sheared undrained at a nominal constant rate of 7 %/day up to 20 % axial strain.

3 RESULTS

3.1 *Microstructure characterisation*

A few SEM images were selected to highlight the soil microstructure in intact and remoulded specimens of both silts. Figure 2 and Figure 3 show the comparison of soil microstructure between intact and remoulded Silt A at 1,500 times magnification. Based on the images, the microstructure of Silt A is composed of a clay matrix made of flocculated clay particles, with silt inclusions (large angular particles). For the intact specimen, a large size microfossil can be seen at the centre of the image, with size approximately 30 μm to 50 μm. The microfossil has a honeycomb structure with intra voids of radius ranging between 3 μm to 5 μm. This type of structure is not visible in the case of the remoulded specimen, suggesting that the microfossil particles may have been crushed during the reconstitution process. The microstructure of the intact specimen appears

quite open with relatively large voids between particles, while for the remoulded specimen, a more compacted structure can be observed, with smaller voids.

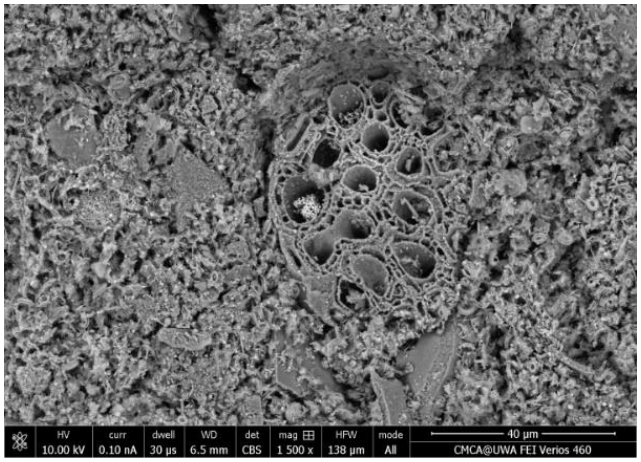

Figure 2: SEM image of intact Silt A

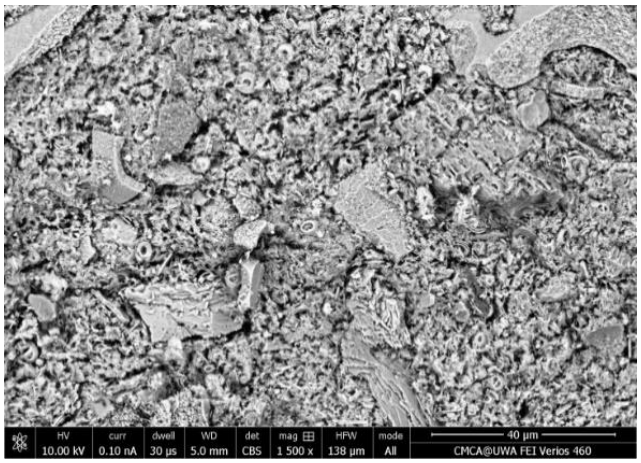

Figure 3: SEM image of remoulded Silt A

Figure 4 and Figure 5 compare the microstructure between intact and remoulded Silt B specimens at 1,500 magnifications. In contrast with Silt A, Silt B does not exhibit a typical clay microstructure, but instead the microstructure is composed of a conglomerate of broken microfossils and elongated and angular particles. From the PSD, Silt B has a higher percentage of clay-size particles compared to Silt A. A large presence of coccoliths can be seen in the intact specimen of Silt B as shown on Figure 4. Coccoliths are microscopic circular plates resulting from the breakage of coccospheres (formed by single-celled algae such as *Emiliania huxleyi*). They are individual chalk plates that contribute to a significant presence of calcium carbonates in this soil. The presence of coccoliths in Silt B is consistent with the water depth of this soil (i.e. 1341 m) as coccoliths are normally found in deeper water. In the case of the remoulded specimen of Silt B, full size coccoliths cannot be seen, which suggests that the coccoliths may have been damaged during the process of reconstituting the specimen. The arrangement of particles in remoulded specimen of Silt B appears to be well distributed with abundant elongated and angular particles. Similarly as intact Silt A, the structure of the intact Silt B appears to be looser with larger voids compared to the remoulded specimen.

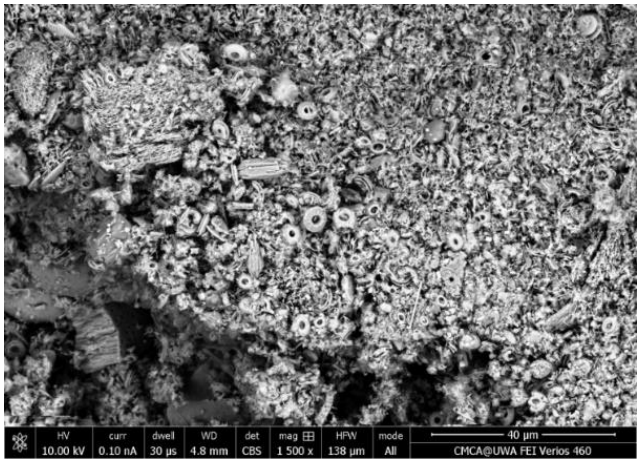

Figure 4: SEM image of intact Silt B

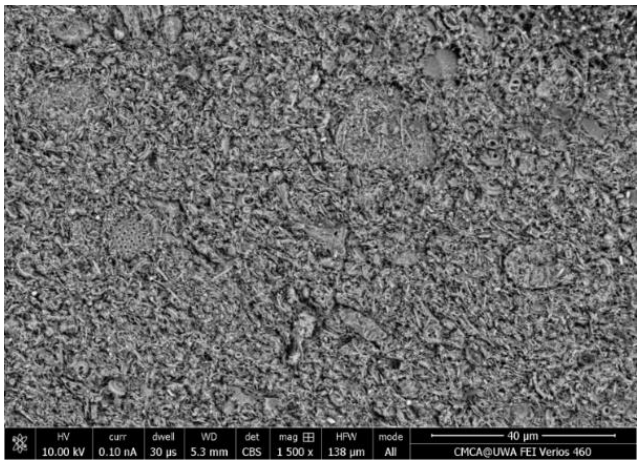

Figure 5: SEM image of remoulded Silt B

Results from XRD show that both silts were composed of mainly calcite, aragonite, halite and alpha quartz (low quartz) with variable percentages. The results are in agreement with previous studies of calcareous sands (Carter et al. 1988; Coop 1990; Coop & Atkinson 1993; Sharma & Ismail 2006).

3.2 *Compressibility*

Figure 6 show the compression curves obtained from CRS tests carried out on intact and remoulded specimens of both silts. The compression parameters determined from the CRS tests results are listed in **Error! Reference source not found.**. Initially, both intact silts exhibit a stiff response at low stress followed by a gradual increase in compressibility until the response becomes almost linear in the e-logσ'_v plot.

However, no sharp bend in the curve is observed at yield stress, indicating that the 'intact' specimens may have been subjected to disturbance during tube sampling or specimen preparation. Silt A has a lower

void ratio compared to Silt B and is less compressible (see Figure 7). Compared to intact specimens, both remoulded silts show a stiffer response (specimen AR and BR).

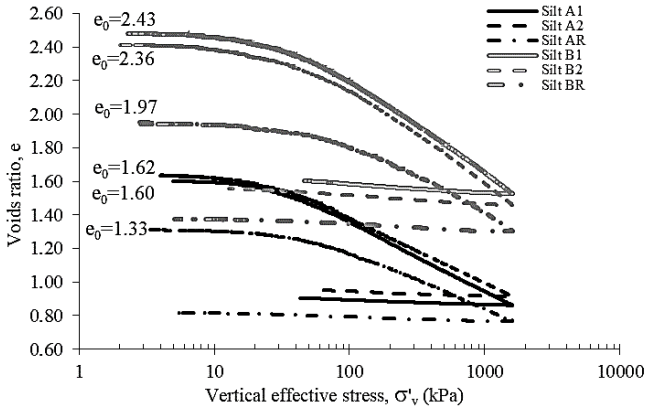

Figure 6: Compression curves of intact and remoulded silts

Figure 7 illustrates the change of compression indices for both soils when compressed to stress levels up to ten times the vertical yield stress, σ'_{yield}. The C_c of both silts falls closely within the range observed for calcarenites (cemented calcareous sands), for which $C_c \sim 0.4 – 0.55$ (Carter et al. 1988). For intact Silt A, once C_c has reached its maximum value of approximately 0.4, it remains stable with increasing effective vertical stress, σ'_v, whereas for remoulded Silt A, C_c increases continuously with increasing σ'_v. However, the range of C_c for both intact and remoulded specimens of Silt A is almost similar. In contrast, for Silt B, C_c is increasing with increasing σ'_v for both intact and remoulded specimens, while the range of C_c values is significantly lower for the remoulded specimen, half the values of intact specimens.

Figure 7: Variation of C_c with normalised effective vertical stress

For both intact silts, the yield stress ratio (YSR = $\sigma'_{yield}/\sigma'_{v0}$) is greater than 1, even though there is no evidence of previous stress loading history for these sediments. 'Apparent' pre-consolidation is a common feature of many offshore clay deposits, which has been attributed by several authors to aging effects (Schmertmann 1991; Puech et al. 2005). Compared to Silt A at the same depth, Silt B which is more fine-grained, exhibits a higher natural void ratio, higher yield stress, higher yield stress ratio and higher compression index. The swelling index, C_s, is similar for both soils and is not affected by the reconstitution process.

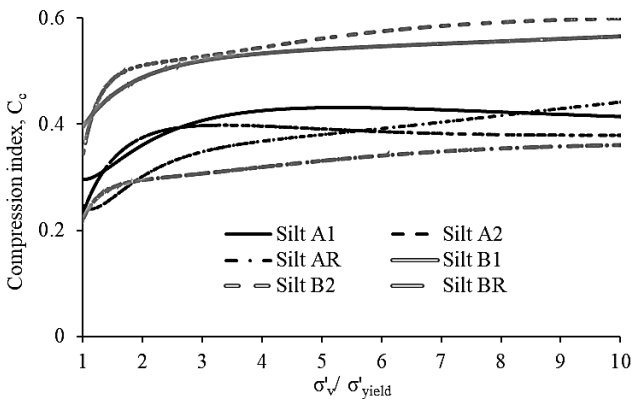

Table 2: Compressibility parameters from CRS tests

Specimen	σ'_{v0} (kPa)	σ'_{yield} (kPa)	$\sigma'_{yield}/\sigma'_{v0}$	C_s
A1	21	35	1.7	0.03
A2	24	36	1.5	0.04
AR	N/A	60	1.0	0.03
B1	13	60	4.6	0.05
B2	16	80	5.0	0.05
BR	N/A	62	1.0	0.05

3.3 *Behaviour in undrained triaxial compression*

The list of triaxial tests carried out is summarised in Table 3. Three tests were conducted on each intact silt, with varying values of vertical consolidation stress, σ'_{vc}. For Silt A, values of σ'_{vc} were selected as follows: (i) close to the *in situ* vertical stress, (ii) close to the yield stress, (iii) significantly larger than the yield stress. A similar logic was followed for Silt B, except for the lowest consolidation stress value, which was selected to be lower than the yield stress, but high enough such that it could be controlled accurately by the loading system (the *in situ* vertical stress was low for this case ≈ 10 kPa).

Table 3: Summary of triaxial compression tests

Silt	e_0	σ'_{vc} (kPa)	σ'_{rc} (kPa)	e_c	ε_{vol} (%)	q_{peak} (kPa):	$\varepsilon_{axial,peak}$ (%)
A1	1.67	20	10	1.59	2.83	21.5	8.9
A2	1.61	35	17.5	1.5	4.51	28	0.4
A3	1.64	70	35	1.39	9.42	58.5	0.3
B1	2.21	35	17.5	2.04	5.14	45.3	12.1
B2	2.41	70	35	2.19	6.3	82.7	12.2
B3	2.5	200	100	2.04	13.27	219.5	8.1
AR	1.33	70	35	1.2	5.35	63.4	0.3
BR	2.01	70	35	1.91	3.44	63.3	6.6

Figure 8 shows the response for intact and remoulded specimens of Silt A during undrained triaxial compression. Specimen A1, which can be considered as "over-consolidated", shows a contractive-dilative behaviour, with the deviator stress increasing monotonically up to its maximum value, whereas the other "normally consolidated" specimens exhibit a contractive response, with the deviator stress reaching a peak before decreasing. The remoulded specimen, AR, reaches higher peak shear strength (8 % higher) compared to the intact specimen consolidated to the same stress level (A3). This is consistent with the higher density (lower void ratio) of the remoulded specimen. Except for A3, all tests reached the same critical state line in the effective stress space.

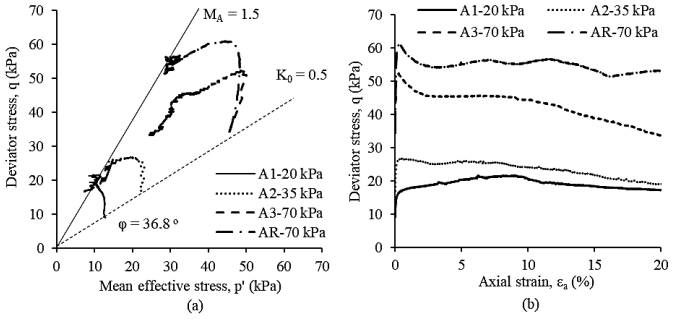

Figure 8: Undrained shearing response of Silt A

Figure 9 presents the undrained shearing response of Silt B. Both Specimens B1 and B2 exhibit a contractive-dilative response with monotonically increasing deviator stress, whereas the "normally consolidated" specimens B3 and BR show a contractive response. Only specimen BR displays a peak deviator stress followed by a gradual drop. In comparison with the intact silt which was consolidated to the same stress level (B2), the remoulded silt, BR reaches a lower peak shear strength (31% lower). The vertical consolidation stress for Silt B2 was selected to be close to the yield stress (around 60 to 80 kPa), however, the shearing response obtained seems to indicate that the specimen may have been "over-consolidated" (similar response as B1). In comparison to Silt A, the peak shear strength for all specimens of Silt B occurs at larger shear strains.

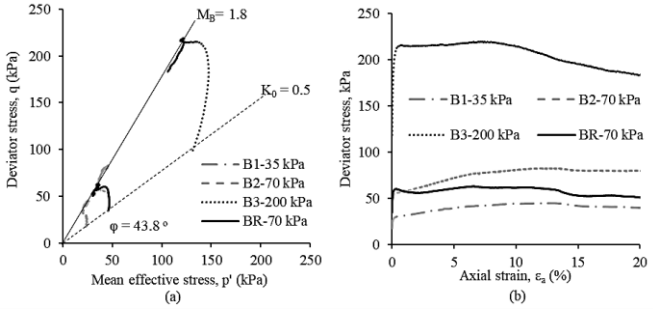

Figure 9: Undrained shearing response of Silt B

Considering the point at which the deviatoric stress stabilises during undrained triaxial compression as the critical state, one can define the critical state friction angle, ϕ'_{cv} ~ 36.8° (M~1.5) for Silt A and ϕ'_{cv} ~ 43.8° (M~1.8) for Silt B as shown in Figure 8 and Figure 9. Silt A has a lower ϕ'_{cv} compared to Silt B, while remoulded specimens of Silt A and Silt B reach the same critical state line as their corresponding intact specimens. Silt B, which has a high calcium carbonate content typical of carbonate soils, has a friction angle that compares well with an average value ϕ'_{cv} = 44.8° reported by Airey & Fahey (1991) for calcareous sands and silts and a value ϕ'_{cv} = 40° reported by Coop (1990) for calcareous sand. Interlocking of broken shell particles may contribute to a higher ϕ'_{cv} for Silt B compared to Silt A.

4 DISCUSSION

Microscopically, two main distinctive characteristics of calcareous soils contribute to their specific behaviour which are: (i) the presence of intra-particle voids, and (ii) irregular shape of particles from microfossils such as coccoliths. These observations were reported also in previous studies (Hyodo et al. 1996; Hyodo et al. 1998; Sharma & Ismail 2006). These characteristics result from various chemical, physical, mechanical, and biological deposition processes of skeletal remains of marine organisms in deep water. Also related to these features is the susceptibility to particle breakages, which affects the compression and shear behaviour of these soils. Similar characteristics can be seen in Silt A and Silt B based on their SEM images. These silts have particles with irregular shapes and sizes, large voids between particles and internal voids within particle. However, the specimen reconstitution process changes the fabrics and arrangements of particles, as shown in the SEM images of remoulded specimens. These changes result in a more compacted arrangement and reduced void ratio. Presence of intra-void within particles, such as void in coccoliths, contributes to the void ratio calculation based on moisture content (Demars 1982). In Silt A and B, this calculation may not be a good indicator to analyse soil behaviour, especially undrained strengths of silts, as suggested by Lehane et al. (2014).

Except for the swelling index, C_s, the compressibility parameters (σ'_{yield} and C_c) are affected by the reconstitution process. Yield stress of the remoulded specimens depends on the maximum stress applied to reconstitute the specimen, whereas in the case of the intact specimens, σ'_{yield} is related to the soil's fabric and possibility to light cementation. Higher σ'_{yield} is observed in Silt B compared to Silt A, with Silt B also having a more fine-grained and open structure particles arrangement. For Silt A, C_c of the remoulded specimen is similar to that of the intact specimens, while for Silt B, C_c of the remoulded specimen is only half of the values determined for the intact specimens. From the series of undrained triaxial compression tests conducted on intact specimens of Silt A and Silt B, the following pattern seems to emerge: over-consolidated specimens ($\sigma'_{vc} < \sigma'_{yield}$) exhibit a contractive/dilative response with strain-hardening (A1, B1 and B2), whereas normally consolidated specimens show a contractive response (A2, A3, B3). The remoulded specimens, which are normally consolidated, also exhibit a contractive response (AR, BR).

It is difficult to replicate the stress-strain response during undrained shearing of intact specimen using

remoulded specimens for both silts. The response depends on the state of the specimens before shearing, i.e., final void ratio and effective stresses, but also on the structure, which differs between intact and remoulded specimens. For comparison between remoulded and intact specimens, AR and BR were consolidated to the same effective stress as A3 and B2, respectively. For Silt A, AR and A3 exhibit a similar contractive behaviour. However, AR has a lower void ratio and different structure than A3, which results in a higher undrained shear strength. For Soil B, B2 and BR display a different behaviour, as B2 appears to be over-consolidated, showing contractive/dilative response and BR shows a contractive behaviour (normally consolidated), which results in a lower undrained shear strength compared to B2. However, remoulded specimens reached the same critical state lines as the intact specimens for both silts, which may suggest some state parameters from remoulded specimens can be used to represent the state parameters of intact specimens. It also suggests that results from physical modelling, which is generally based on remoulded samples, may be directly applicable to intact soil in the cases that are governed by the critical state parameter M.

5 CONCLUSION

Based on the results of this study, the following enhancement of our understanding on offshore calcareous soils can be concluded:

a. The percentage of microfossils (which relates to the percentage of calcium carbonate) in soil structure and fabrics increases with water depth, as shown in SEM images.
b. Important characteristics of calcareous soils, such as large intra-voids within particles and irregular particles shapes and sizes contribute to soil compressibility and behaviour during undrained shearing (such as high friction angle).
c. The type of undrained shearing response, i.e., contractive/dilative or contractive appears to be correlated with the initial state of the soil at the end of consolidation, i.e., over-consolidated or normally consolidated. The critical state parameters such as the slope of the critical state line (or friction angle) are well reproduced using remoulded specimens.

Further investigations are required to establish a proper framework for fine-grained calcareous soils and refined guidance on the applicability of using remoulded specimens to represent the behaviour of intact specimens.

REFERENCES

Airey, D.W. and Fahey, M., 1991. Cyclic response of calcareous soil from the North-West Shelf of Australia. *Géotechnique*, *41*(1), pp.101-121.

Anantanasakul, P, Yamamuro, JA & Kaliakin, VN 2012, 'Stress-strain and strength characteristics of silt-clay transition soils', Journal of Geotechnical and Geoenvironmental Engineering, vol. 138, no. 10, pp. 1257-1265.

Carter, J, Johnston, I, Fahey, M, Chapman, G, Novello, E & Kaggwa, W 1988, 'Triaxial testing of North Rankin calcarenite', Engineering for Calcareous Sediments, vol. 2, pp. 515-53.

Cola, S & Simonini, P 2002, 'Mechanical behavior of silty soils of the Venice lagoon as a function of their grading characteristics', Canadian Geotechnical Journal, vol. 39, no. 4, pp. 879-893. [2018/03/22].

Coop, M 1990, 'The mechanics of uncemented carbonate sands', *Géotechnique*, vol. 40, no. 4, pp. 607-626.

Coop, M & Atkinson, J 1993, 'The mechanics of cemented carbonate sands', *Géotechnique*, vol. 43, no. 1, pp. 53-67.

Demars, KR 1982, 'Unique engineering properties and compression behavior of deep-sea calcareous sediments', in Geotechnical properties, behavior, and performance of calcareous soils, ASTM International.

Hyodo, M, Aramaki, N, Itoh, M & Hyde, AFL 1996, 'Cyclic strength and deformation of crushable carbonate sand', Soil Dynamics and Earthquake Engineering, vol. 15, no. 5, pp. 331-336.

Hyodo, M, Hyde, AFL & Aramaki, N 1998, 'Liquefaction of crushable soils', *Géotechnique*, vol. 48, no. 4, pp. 527-543.

Lehane, BM, H. Carraro, JA, Boukpeti, N & Elkhatib, S 2014, 'Mechanical response of two carbonate sediments from Australia's North West Shelf', no. 45411, p. V003T10A008.

Mao, X & Fahey, M 2003, 'Behaviour of calcareous soils in undrained cyclic simple shear', *Géotechnique*, vol. 53, no. 8, pp. 715-727.

McClelland, B 1988, 'Calcareous sediments: an engineering enigma', in Proc. 1st Int. Conf. on Calcareous Sediments, Perth, Australia, pp. 777-784.

Murthy, TG, Loukidis, D, Carraro, JAH, Prezzi, M & Salgado, R 2007, 'Undrained monotonic response of clean and silty sands', *Géotechnique*, vol. 57, no. 3, pp. 273-288.

Nyland, G 1988, 'Detailed engineering geological investigation of North Rankin 'A'platform site', in Proc. Int. Conf. Calcareous Sediments, pp. 503-512.

Price, GP 1988, 'Fabric of calcareous sediments at North Rankin A, North West Shelf', in International Conference of Calcareous Sediments, Rotterdam:Balkema, Perth.

Puech, A, Colliat, J, Nauroy, J & Meunier, J 2005, 'Some geotechnical specificities of Gulf of Guinea deepwater sediments', in Proceedings of the International Symposium on Frontiers in Offshore Geotechnics, Perth, Australia, pp. 1047-1053.

Schmertmann, JH 1991, 'The mechanical aging of soils', Journal of Geotechnical Engineering, vol. 117, no. 9, pp. 1288-1330.

Sharma, SS & Ismail, MA 2006, 'Monotonic and cyclic behavior of two calcareous soils of different origins. ', Journal of Geotechnical and Geoenvironmental Engineering, vol. 132, no. 12, p. 1581.